International Journal of Thermophysics, Vol. 20, No. 2, 1999

Measurement of Specific Heat Capacity from 150 to 310 K by Thermal Radiation Calorimetry

S. Sawai,[1,2] H. Tanaka,[1] K. Morimoto,[1] and K. Hisano[1]

Received July 29, 1998

A novel method for measurement of the specific heat capacity in the temperature range from 150 to 310 K is described. In order to achieve good temperature homogeneity in a disk-shaped specimen, a cylindrical heater was used in an apparatus based on thermal radiation calorimetry. A mixture of Bi_2O_3 and MgO powders was used for blackening the surfaces of the specimen, the heater, and the inside wall of the chamber. The specific heat capacities of Ni, fused quartz glass, and $BaTiO_3$ ceramic were measured to test the performance of the calorimeter. Agreement to within 5% of the values published in the literature was obtained for these samples. Thermal hysteresis and anomalies associated with the first-order phase transition in $BaTiO_3$ were detected in the present experiment.

KEY WORDS: effective emissivity; specific heat capacity; thermal radiation calorimetry.

1. INTRODUCTION

Thermal radiation calorimetry (TRAC) was previously developed for measurement of the specific heat capacity in the high temperature range from 200 to 500°C [1]. In this method, a disk-shaped specimen is heated and cooled only by thermal radiation from a heater (or cooler) in a vacuum chamber. The radiant power exchanged between the heater, the specimen, and the wall of the chamber is evaluated, and the specific heat capacity is obtained only from their temperatures and the time rate change of the

[1] Department of Mathematics and Physics, National Defense Academy, Hashirimizu 1-10-20, Yokosuka 239-8686, Japan.

[2] To whom correspondence should be addressed.

0195-928X/99/0300-0721$16.00/0

specimen temperature. These surfaces are blackened with high-emissivity material to achieve the same high emissivity for all measured specimens. However, in the previous system, the disk-shaped specimen was heated only on one face by radiation from a flat heater. This means that for a relatively thick, thermally insulated specimen, there may be a temperature gradient through the specimen even though the measurement is performed at low temperatures [2, 3].

A technique for measurement of the specific heat capacity in the temperature range from 150 to 310 K is presented in this paper. The specimen is set inside a cylindrical resistive heater so that good temperature homogeneity is achieved. A powder mixture of Bi_2O_3 and MgO is used for blackening the specimen surfaces. This material provides high emissivity in the low temperature range. The specific heat capacities of Ni metal, fused quartz glass, and $BaTiO_3$ ceramic are measured in the temperature range from 150 to 310 K, and these values are compared with those published in the literature.

2. PRINCIPLES OF THERMAL RADIATION CALORIMETRY

When a disk-shaped specimen (mass M, surface area A, specific heat capacity C_p) is heated and cooled only by thermal radiation from a heater (cooler) in a vacuum chamber, the time rate change of the specimen temperature, dT_s/dt, is described by

$$MC_p \frac{dT_s}{dt} = E_h A(I_h - I_s) - E_s A(I_s - I_w) - \frac{dQ_s}{dt} \tag{1}$$

where I is the emissive power of blackbody radiation, which is equal to σT^4 (σ is the Stefan–Boltzmann constant and T is temperature). Subscripts s, h, and w refer to the specimen, the heater, and the wall of the vacuum chamber, respectively. dQ_s/dt is the conductive heat loss per unit time through thermocouple leads, etc. E_h is the *effective emissivity* arising from the radiant heat transfer between the specimen and the heater. Similarly, E_s corresponds to that between the specimen and the chamber wall. These effective emissivities are constant as long as the geometric configuration between the heater and the specimen in the chamber and the emissivities of these surfaces are the same and independent of temperature. The validity of Eq. (1) was confirmed by calculations based on the net-radiation method [3, 4]. In a typical experimental run, the specimen is heated gradually over a certain temperature range and then cooled over the same range. T_w is kept constant during the experiment. The specific heat capacity C_p is

derived from Eq. (1) at the same specimen temperature T_s for the heating process (i) and the cooling process (d):

$$\frac{C_p}{E_h} = \frac{A(I_{hi} - I_{hd})}{M((dT_{si}/dt) - (dT_{sd}/dt))} \tag{2}$$

where $dQ_{si}/dt = dQ_{sd}/dt$ at the same T_s. If E_h is evaluated experimentally with the standard sample, the heat capacity $C_p(T_s)$ can be estimated.

At thermal equilibrium, Eq. (1) becomes

$$E_h A(I_{h0} - I_s) - E_s A(I_s - I_w) - \frac{dQ_{s0}}{dt} = 0 \tag{3}$$

where $I_{h0} = \sigma T_{h0}^4$, and T_{h0} is the temperature of the heater in the equilibrium state. When thermal hysteresis is observed between the heating and the cooling processes, C_p is obtained from the following equation, given by substituting Eq. (3) into Eq. (1):

$$MC_p \frac{dT_s}{dt} = AE_h(I_h - I_{h0}) \tag{4}$$

where $dQ_{s0}/dt \simeq dQ_s/dt$. In this case, we have to know T_{h0} in order to estimate C_p. Equation (4) is rewritten as

$$I_{h0} = I_h - \frac{MC_p}{AE_h}\frac{dT_s}{dt} \tag{5}$$

T_{h0} is assumed to be a function of T_s. Outside the anomalous region, T_{h0} can be calculated by the following equation, given by the substitution of Eq. (2) into Eq. (5):

$$T_{h0}^4 = \frac{T_{hd}^4(dT_{si}/dt) - T_{hi}^4(dT_{sd}/dt)}{(dT_{si}/dt) - (dT_{sd}/dt)} \tag{6}$$

3. EXPERIMENTAL

A schematic diagram of the experimental setup is shown in Fig. 1. A disk-shaped specimen (20 to 25 mm in diameter, 2 to 3 mm thick) was suspended by an acrylic rod (1 mm in diameter, 25 mm long) within a cylindrical resistive heater (37-mm inside diameter, 50 mm high). The specimen and the heater were placed in a vacuum chamber, which was immersed in a liquid nitrogen bath in order to keep the temperature of the

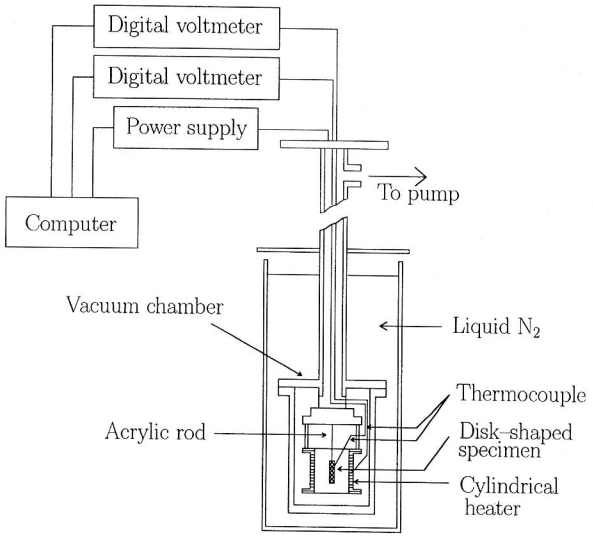

Fig. 1. Schematic diagram of the thermal radiation calorimeter used for measurements in the temperature range of 150 to 310 K. A specimen is suspended inside the cylindrical heater in the vacuum chamber. The temperature of the chamber wall is maintained at liquid nitrogen temperature.

chamber wall at liquid nitrogen temperature. The chamber (57.5-mm inside diameter, 135 mm high) was evacuated to 10^{-3} Pa during the measurement. The temperature of the heater, T_h, was measured by a copper–constantan thermocouple (0.1 mm in diameter) which was attached to the cylindrical heater. A chromel–alumel thermocouple (0.1 mm in diameter) was inserted in a hole (0.75 mm in diameter, 7 mm depth) drilled in the side surface of the specimen to measure the specimen temperature, T_s. The surfaces of all specimens, the heater, and the inside wall of the chamber were coated with a mixture of Bi_2O_3 and MgO powders (2:1 weight ratio) for blackening. The emission spectrum of the powder, which was coated on a copper plate, was measured by a Brucker 113v FT-IR spectrometer to confirm its high emissivity [5]. The heater current was controlled so that the time rate change of the specimen temperature was maintained in the range from 0.5 to 2.7 $K \cdot min^{-1}$. Temperature data, T_s and T_h, were collected every 15 s with a personal computer. A copper disk-shaped specimen was used as a reference material to obtain the value of E_h in the temperature range from 150 to 310 K since its thermal conductivity is relatively high and its specific heat is relatively well established in this range [6]. Specimens of polycrystalline Ni metal and fused quartz glass were prepared

to confirm the reliability of the present calorimeter. $BaTiO_3$ ceramic, which was synthesized by Hayashi Chemicals (Kyoto) and contains 64.5 wt% BaO and 34.4 wt% TiO_2, was also prepared, and anomalies associated with the first-order phase transition were measured.

4. RESULTS AND DISCUSSION

4.1. Effective Emissivity E_h

Figure 2 shows the emission spectrum of the mixture of Bi_2O_3 and MgO powders (2:1 weight ratio) at 420 K in the wavelength range from 5 to 200 μm. The spectral emissivity, $\varepsilon(\lambda)$, is 0.8 to 1.0 in the range from 6 to 150 μm. The hemispherical emissivity, ε, was estimated from the following equation, assuming that Lambert's law holds because of the high spectral emissivity and rough surface,

$$\varepsilon = \frac{\int_{3\,\mu m}^{200\,\mu m} \varepsilon(\lambda)\, W(\lambda, T)\, d\lambda}{\int_{3\,\mu m}^{200\,\mu m} W(\lambda, T)\, d\lambda} \tag{7}$$

$$\approx \frac{\int_{3\,\mu m}^{200\,\mu m} \varepsilon(\lambda)\, W(\lambda, T)\, d\lambda}{\sigma T^4} \tag{8}$$

where $W(\lambda, T)$ is Planck's emissive power. The calculated results of ε are shown in Fig. 3. For this calculation, $\varepsilon(\lambda)$ between 3 and 5 μm was assumed to be the same at 5 μm taking account of the spectral absorptivity at room

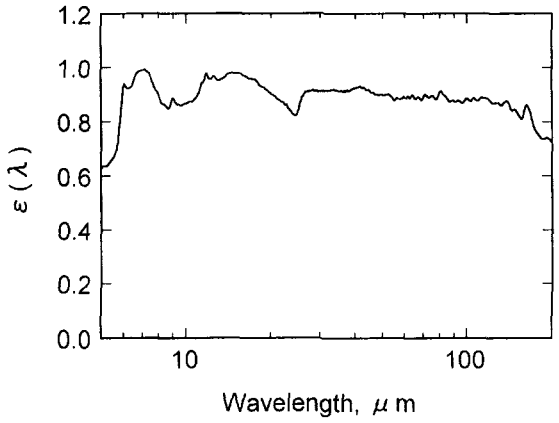

Fig. 2. Spectral emissivity of the mixture of Bi_2O_3 and MgO powders at 420 K.

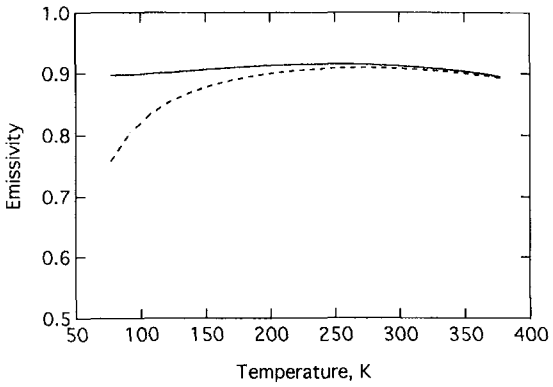

Fig. 3. Hemispherical emissivities of the mixture of Bi_2O_3 and MgO powders calculated from Eqs. (7) and (8), represented by the solid and the dashed line, respectively.

temperature. The lower line (dashed) indicates the result obtained from Eq. (8), while the upper line (solid) indicates that obtained from Eq. (7). This discrepancy is caused by the lack of data of $\varepsilon(\lambda)$ beyond 200 μm. The actual value must be between the two lines.

The hemispherical emissivity ε, which was calculated from $\varepsilon(\lambda)$ at 420 K, is fairly constant in the range from 150 to 350 K. Because of the temperature

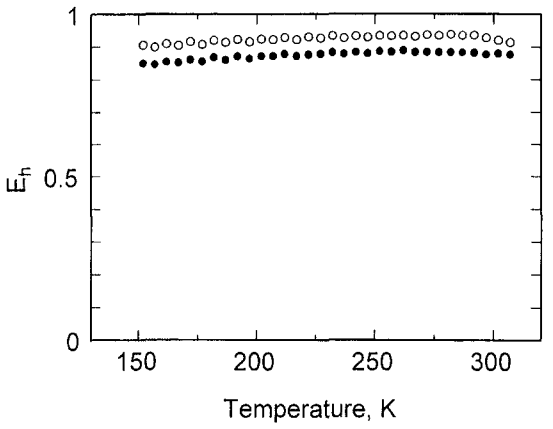

Fig. 4. Temperature dependence (150 to 310 K) of the effective emissivity E_h obtained from the experiment with Cu samples (open circles, diameter of 20 mm; filled circles, diameter of 25 mm).

dependence, it is necessary to know the emission spectra at a lower temperature to obtain a more accurate emissivity. However, the quantity necessary to obtain the specific heat is the effective emissivity E_h, which can be determined experimentally as described below. The determination of the value of the "effective" emissivity between the specimen and the heater, E_h, was performed by measurement of two copper specimens of different diameters, 20 and 25 mm, and common thickness, 2 mm. Figure 4 shows the temperature dependence of E_h for these specimens. E_h is more or less constant with temperature in the range of 150 to 310 K. For the Cu samples with diameters of 20 and 25 mm, the values of E_h were 0.92 ± 0.02 and 0.87 ± 0.02, respectively.

4.2. Specific Heat Capacities of Ni, Fused Quartz Glass, and $BaTiO_3$

Figures 5 and 6 show the temperature dependence of the specific heat capacity of Ni and fused quartz glass, respectively. The solid lines indicate values from the literature [7, 8]. Deviations from those values were within 5% for both specimens. The relative error involved in the values estimated from Eq. (2) is about $\pm 7\%$ in the present measurements.

Figure 7 shows the temperature dependence of dT_s/dt for the measurement of the specific heat of $BaTiO_3$. The two types of anomaly associated with the first-order phase transition are displayed for each process. Figure 8 shows the values of T_{h0} estimated from Eq. (6). Because Eq. (2), that is, Eq. (6), is not valid in the transition region, the anomalies of T_{h0} are displayed and these values of T_{h0} are not in this region. As shown in Fig. 8,

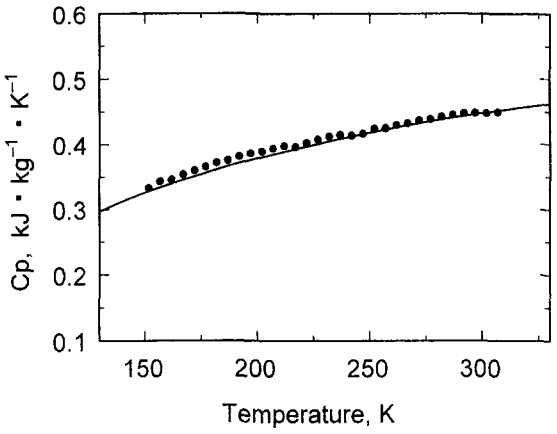

Fig. 5. Specific heat capacity of Ni. The solid line indicates values published in the literature [7].

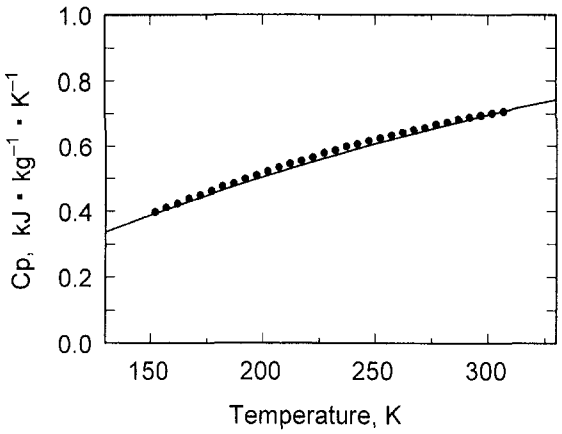

Fig. 6. Specific heat capacity of fused quartz glass. The solid line indicates values published in the literature [8].

the data of T_{h0} fit a straight line rather well outside the anomalous region. The actual values of T_{h0} in the anomalous region were estimated by linear interpolation. Figure 9 shows the temperature dependence of C_p for $BaTiO_3$ obtained by the above estimation of T_{h0} and Eq. (4). The thermal hysteresis in C_p is displayed, and anomalies of C_p associated with the first-order phase transition are observed at two temperatures, T_{c1} and T_{c2}, for

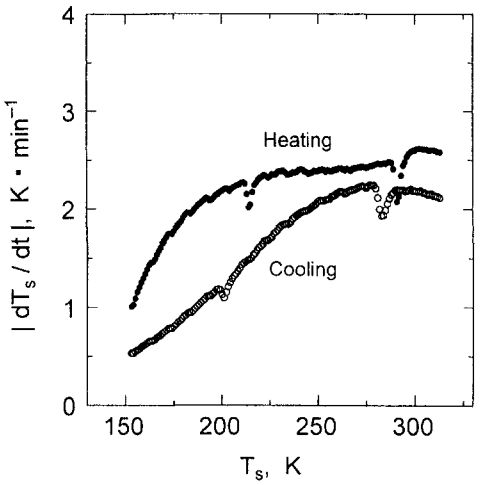

Fig. 7. Temperature dependence of dT_s/dt of a $BaTiO_3$ specimen.

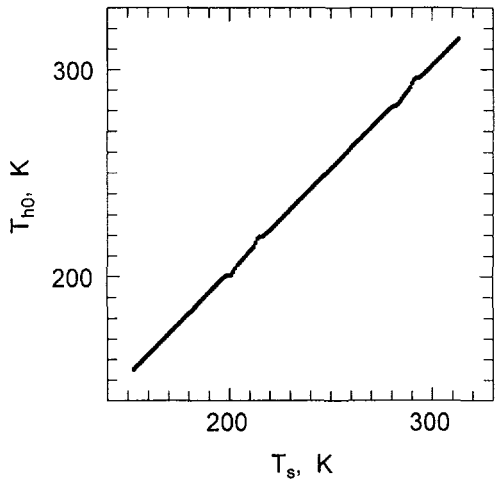

Fig. 8. T_{h0} versus T_s for a $BaTiO_3$ specimen.

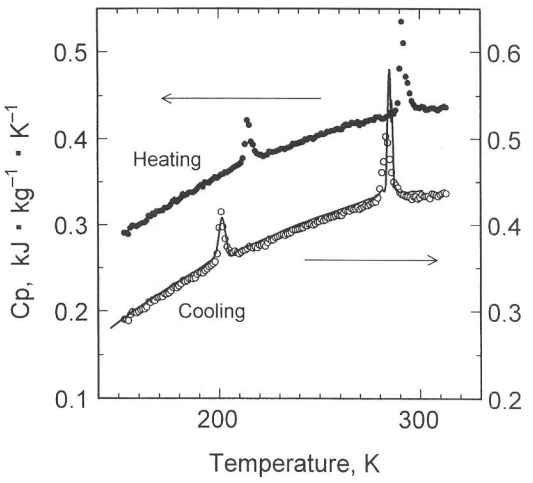

Fig. 9. Temperature dependence of the specific heat capacity of $BaTiO_3$. The filled circles refer to the heating process, and the open circles refer to the cooling process. The solid line indicates the values of Todd and Lorenson [9].

Table I. Values of T_{c1} and T_{c2}

	T_{c1} (K)	T_{c2} (K)
Heating process	214	291
Cooling process	200	283
Todd and Lorenson [9]	201.6	284.9
Shirane and Takeda [10]	200	289

both heating and cooling. The solid line indicates the data of Todd and Lorenson [9]. Table I lists the mean values of T_{c1} and T_{c2} along with previous data [9, 10]. The scatter in the results of each run was ± 2 K. The differences of T_{c1} and T_{c2} between the two processes, ΔT_{c1} and ΔT_{c2}, were estimated at 14 and 8 K, respectively. These agree to some extent with those from the study of the temperature dependence of the dielectric constant of $BaTiO_3$ single crystals by Merz [11], $\Delta T_{c1} \simeq 16$ K and $\Delta T_{c2} \simeq 12$ K.

In the present method, the specific heat in the temperature range of 150 to 310 K is measured in a straightforward manner in a relativly short time, and the specific heat anomaly associated with a phase transition is detected. The costs of the construction and operation of the apparatus are very low.

5. CONCLUSION

Measurement of the specific heat capacity in the temperature range from 150 to 310 K was performed by an apparatus based on thermal radiation calorimetry. The values of the specific heat capacities of Ni, fused quartz glass, and $BaTiO_3$ were obtained and fair agreement, within 5% of the values published in the literature, was obtained for these samples. Thermal hysteresis in the heat capacity of $BaTiO_3$ was displayed, and anomalies due to the first-order phase transition were detected at two temperatures for both heating and cooling. The relative error involved in the measured value was estimated to be $\pm 7\%$. These results indicate that thermal radiation calorimetry is reliable for measuring the specific heat capacity both in the high temperature range and in the lower temperature range from 150 to 310 K.

ACKNOWLEDGMENT

The authors wish to thank Dr. Frank Placido for many helpful discussions.

REFERENCES

1. K. Hisano and T. Yamamoto, *High Temp.-High Press.* **25**:337 (1993).
2. K. Hisano, S. Sawai, and K. Morimoto, *Int. J. Thermophys.* **19**:291 (1998).
3. K. Hisano, S. Sawai, and K. Morimoto, *Int. J. Thermophys.* **19**:305 (1998).
4. R. Siegel and J. R. Howell, *Thermal Radiation Heat Transfer* (McCraw-Hill, New York, 1967).
5. A. Aoki, H. Tanaka, and K. Hisano, in *Proc. 12th Japan Symp. Thermophys. Prop., Vol. 12* (Japan Soc. Thermophys. Prop., Kyoto, 1991), p 9.
6. R. C. Weast (ed.), *CRC Handbook of Chemistry and Physics*, 59th ed. (CRC Press, Boca Raton, FL, 1979).
7. D. E. Gray (ed.), *American Institute of Physics Handbook* (McGraw-Hill, New York, 1972).
8. Y. S. Touloukian and E. H. Buyco, *Thermophysical Properties of Matter 5, Nonmetallic Solids, Specific Heat* (Plenum, New York, 1972).
9. S. S. Todd and R. E. Lorenson, *J. Am. Chem. Soc.* **74**:2043 (1952).
10. G. Shirane and A. Takeda, *J. Phys. Soc. Jpn.* **7**:1 (1952).
11. W. J. Merz, *Phys. Rev.* **76**: 1221 (1949).